OBSERVATION OF DYNAMIC BEHAVIOR OF BURIED PIPELINES DURING EARTHQUAKES

Toshiyuki IWAMOTO (I)
Nobuhiko WAKAI (I)
Tadao YAMAJI (I)
Presenting Author: Toshiyuki IWAMOTO

SUMMARY

We have been observing the dynamic behavior of pipelines and ground movement during earthquake at three sites since 1975. Pipelines are stressed by ground strain, but the pipe stress is eliminated by the sliding movement at pipe joint. Ground strain is generated by the relative displacement of the ground which is produced by the apparent propagation of seismic wave. The apparent phase velocity of seismic waves near the ground surface is related to the velocity of deeper layer of ground, and the seismic behavior of the ground may be estimated by the propagation of the lower three modes of the Rayleigh waves.

INTRODUCTION

We have been observing the behavior of earthquake-proof ductile iron pipeline during earthquake at 3 observation stations in Hachinohe City in the northern part of Honshu Island, Japan, as shown in Fig. 1 — the Kansen site (established in May, 1975), the Hakusan site (established in May, 1975), and the Shimonaga site (established in August, 1977). Individual records of the three observation stations can be synchronized using a time code generator automatically calibrated by the NHK (Japan Broadcasting Corp.) timecast. This report deals with the records of observations made at the Shimonaga observation station. In Addition to the behavior of the pipeline we have also analyzed the ground strain and propagation velocity of seismic waves. The pipe used in observation is an S-type ductile iron pipe 6m long and is shown in Fig. 2. This pipe has a joint that is flexible to expansion, contraction, and deflection and also has an anti-slipout mechanism. At present, this joint is installed in many cities for the countermeasure to earthquake and soft ground.

OBSERVATION EQUIPMENT AND PIPING

(1) Kansen observation station (pipe nominal diameter 1500mm)

As shown in Fig. 3, the measuring instruments are installed at three separate locations along a straight section of the pipeline at intervals of 48m. For ground measurements, seismometers (acceleration, velocity: X, Y directions) and strain gauges (X direction) are set at the pipeline level, and a seismometer (acceleration: X, Y direction) is set at a depth of 25.6m below ground surface level. For measurements of the pipeline itself, an accelerometer for the pipe (X, Y, Z directions), strain gauges for the pipe body (up, down, left, right) and expansion-contraction gauges at the joints (relative displacement gauges across joints, 3 places) are installed.

(I) Pipe Research Department, Kubota Ltd., Hyogo, Japan

In total there are 53 channels making simultaneous measurements at different points. The station is equipped with an emergency power supply.

(2) Hakusan observation station (pipe nominal diameter 1200mm)

As shown in Fig. 4, measurements of the ground are made by a seismometer (acceleration, velocity, displacement: X, Y direction) positioned at the pipeline level, another seismometer (acceleration: Y direction) placed at a depth of 27m below the ground surface, and an accelerometer (X, Y, Z directions) installed in a distributing reservoir. For measurements of the pipeline itself, in addition to an accelerometer (X, Y, Z directions), expansion-contraction gauges at the joints are installed at the connection points to structures, e.g. distributing reservoir, valve box, etc. (3 places), at the bend portions (2 places) and along the straight pipe portions (2 places). In total, there are 31 channels making simultaneous measurements at different points. The station is also equipped with an emergency power supply.

(3) Shimonaga observation station (pipe nominal diameter 1000mm)

As shown in Fig. 5, the Shimonaga observation station has points A and B spaced 60 meters apart on the pipeline as points for observation, and also has point C, the vertex of a regular triangle with line A-B as one side. For ground measurements, the triangular arrangement (points A, B, C) of seismometers (acceleration, velocity, displacement: X, Y directions) are placed at the pipeline level, strain gauges for the ground are placed at points A and B, and seismometers (acceleration: X, Y directions) are also placed at a depth of approximately 45m below the ground surface.
For measurements of the pipeline itself, accelerometers (X, Y directions) are installed at points A, B; strain gauges (left, right) are installed at the pipe; and expansion-contraction gauges are installed at the joints (4 places). In total there are 42 channels making simultaneous measurements in different points. The station is also equipped with an emergency power supply.

ANALYZED DATA and GROUND MODEL

38 earthquakes have been recorded at Shimonaga observation station since the start of observation in August, 1977. From those, 2 earthquake records were elected for analyses, as shown in Table 1.
Record of No.1 is the biggest earthquake to hit the area since the start of observation.

As shown in Fig. 5, the ground at Shimonaga observation station is composed of layers of humus, soft sand, and silt. The basement is approximately 40m deep, making it a typically stratified soft ground structure.
The predominant period of this ground is about 1 second. (Ref. 1)
The deep underground structure along Hachinohe Bay as shown in Fig. 1 was investigated by Sakajiri et al. (Ref. 2).
The ground structure for points 1 - 8 is shown in Fig. 6.
Since the Shimonaga observation station is parallel to ground point 6, the ground model, including the deep section which was estimated from the PS nogging at points shown in Fig. 5 and ground model shown in Fig. 6 is shown in Fig. 7. Fig. 8 shows the theoretical dispersion curves of the phase and group velocities of the Rayleigh wave based on ground model shown in Fig. 7.

BEHAVIOR OF GROUND AND PIPELINE

The recorded waves of the Miyagiken-oki earthquake (No.1 in Table 1) are shown in Fig. 9. Fig. 10 shows the relationships between the ground strain and the expansion-contraction at the joint and between ground strain and pipe strain in this wave.
From these figures, the followings were determined.

(1) The deformation behavior of the ground, such as tension and compression, is apparent from the ground strain wave.

(2) Because each wave of the ground strain, pipe strain, and expansion-contraction at joint are of the same phase, we have determined that the pipeline is subject to force from the ground strain.

(3) The expansion-contraction at joint increases with the ground strain. In contrast, the pipe strain does not increase beyond a certain amount. Therefore, it is clear that the joint is releasing the force loaded to the pipe by the ground strain. The same fact was observed at Kansen observation station as shown in Fig. 3.

GROUND STRAIN AND PROPAGATION VELOCITY OF SEISMIC WAVES

Fig. 11 shows the waves of velocity amplitude of ground (X direction) measured at points A, B and C during Miyagiken-oki earthquake (No.1 in Table 1). The wave forms are almost identical, but the phases lag slightly behind each other. The comparison between calculated ground strain wave and the measured ground strain wave is shown in Fig. 12. The calculated ground strain wave (ε) is obtained by equation (1) using the velocity waves (v) at points A and B (ℓ=60m apart along the pipe axis X direction) in Fig. 5.

$$\varepsilon = \int (v_B - v_A)\, dt/\ell \qquad (1)$$

The phases and amplitudes of strain coincide almost exactly. Therefore it is determined that ground strain was generated by the phase difference between those two points, and the phase difference resulted from the propagation of seismic waves from point A to B.
(The measured ground strain shown in Fig. 12 is calculated by dividing the wave of expansion-contraction at joint shown in Fig. 9 by pipe length 6m).
Fig. 13 shows the same analyzed result for record of No. 2 in Table 1. Result of No. 2 is almost the same result as No. 1. We tried 2 methods for analyzing the propagating (phase) velocity (V) of seismic waves between points A and B.

(1) The $V = v/\varepsilon$ method of dividing the velocity amplitude (v) by ground strain (ε) to obtain the Fourier spectrum of V values.

(2) The phase difference method which obtains the result from the differences between the Fourier phase spectra of the waves of each of the two points.

The propagation velocity (phase velocity) from A to B obtained by methods (1) and (2) is shown in Figs. 14 and 15. It is apparent from Figs. 14 and 15 that methods (1) and (2) give almost identical results.

We tried to superimpose the theoretical dispersion curves on the results of 2 methods. The theoretical dispersion curve are phase velocity of the Rayleigh waves (Fig. 8) and Love waves for ground model shown in Fig. 7. See Figs. 14 and 15.
From those, the measured result seems to match the phase velocity of the Rayleight wave, which takes into consideration the deep section of the ground. This considers not only the fundamental mode but also the modes of higher order, i.e., the first to the third order.
Ground strain (ε) is calculated by the equation (2) using the measured velocity amplitude (v) at the point A and the phase velocity (V) of the Rayleigh wave in Fig. 8.

$$\varepsilon = v/V \qquad (2)$$

The results are shown in Figs. 16 and 17. The Fourier spectra for the measured ground strain wave and each calculated ground strain wave are also shown in Figs. 16 and 17. The measured wave coincides with the calculated waves that take into consideration not only the fundamental mode but also higher order modes in order.

CONCLUSIONS

(1) Pipe strains are primarily caused by ground strains. However, ductile iron pipe, having the high strength and capability of expansion-contraction at joints, almost completely eliminate the pipe strains.

(2) Ground strain may be estimated from the relative displacement computed by the displacement time histories of two points some distance apart, and such relative displacement is produced by the apparent propagation of seismic waves.

(3) The apparent phase velocity of seismic waves near the ground surface is related to the velocity of deeper layers of ground. And the seismic behaviors of the ground near the surface may be estimated by assuming the propagation of the lower three modes of the Rayleigh waves for layers which are from depth of about 400m to the ground surface.

This report has dealt with the results of analyses of the records of earthquake of middle distance at the Shimonaga observation station. More detailed analyses are planned for records of near earthquake. These observations were supported by the Water Dept. of Hachinohe Municipality, and we sincerely thank them for their kind assistance.

REFERENCES

(1) Iwamoto, T. Wakai, N. Yamaji, T. Nagao, S., "Observation of Dynamic Behavior of Buried Ductile Iron Pipelines During Earthquakes", 4th National Congress on Pressure Vessel & Piping Technology, ASME, 1983.

(2) Sakajiri, N. et al., "Observation of 1-to 5-sec Microtremors and Their Application to Earthquake Engineering. Part I; Preliminary Observation in Hachinohe City.," Faculty of Engineering, Hokkaido University, Vol. 27, 2nd ed., (1974), p. 338-351.

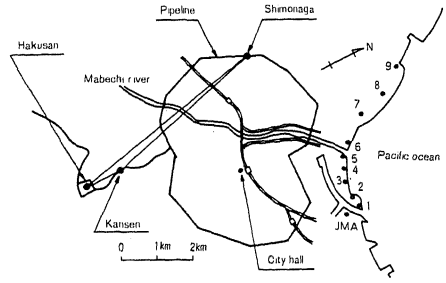

Fig. 1. Position of observation station (Hachinohe City, Japan)

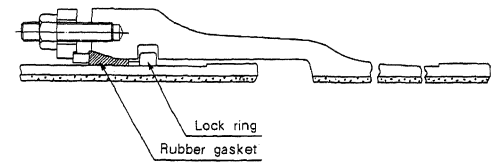

Fig. 2. S-type joint (Ductile Iron pipe)

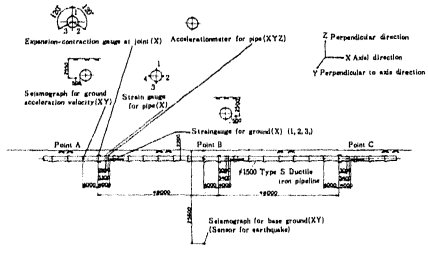

Fig. 3. Kansen observation station

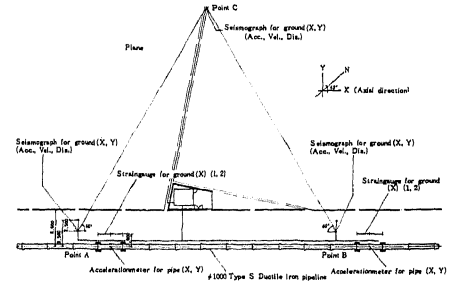

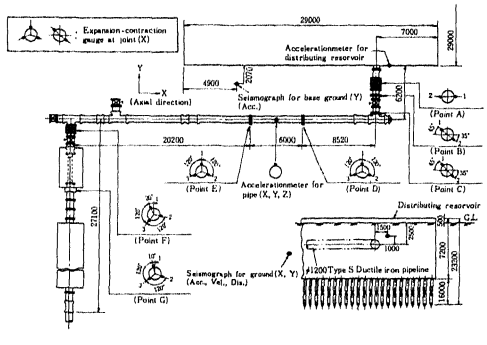

Fig. 4. Hakusan observation station

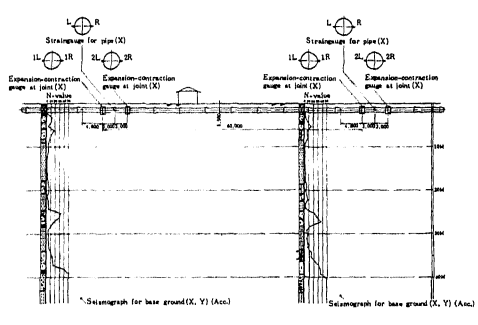

Fig. 5. Shimonaga observation station

Table 1. Analyzed earthquake records (Shimonaga)

No.	LOCATION	DATE	EPICENTER	Mag.	DEPTH (km)	JMA INTENSITY SCALE	Max. Acc(X) (gal)	DISTANCE (km)
1	MIYAGIKEN-OKI	1978. 6.12 17:14	142°10′E 38°09′N	7.4	40	IV	125.1	271
2	MIYAGIKEN-OKI	1978. 6.14 20:34	142°29′E 38°21′N	6.3	40	II	14.8	257

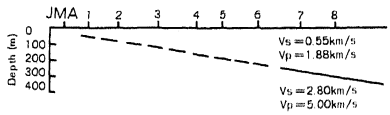

Fig. 6. Ground model (points 1-8 in Fig. 1.)

V_p (m/sec)	V_s (m/sec)	ρ (gf/cm³)	H (m)	Depth (m)
280	40	1.35	2	0
670	40	1.35	1	2
670	60	1.30	2	3
1450	180	1.65	4	5
1450	110	1.45	9	9
1450	160	1.60	7	18
1450	235	1.90	4	25
1450	170	1.55	5	29
1450	270	1.80	7	34
2300	470	2.10	159	41
5000	2800	2.60	∞	200

Fig. 7. Ground model (Shimonaga)

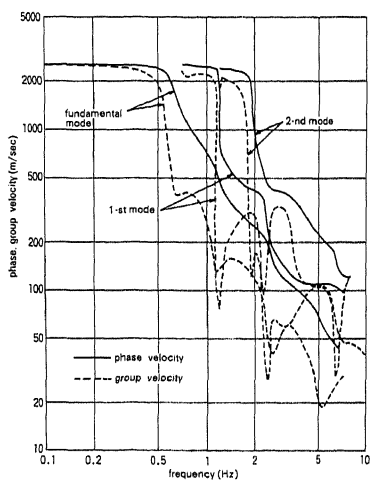

Fig. 8. Dispersion curve of Rayleigh wave (Shimonaga)

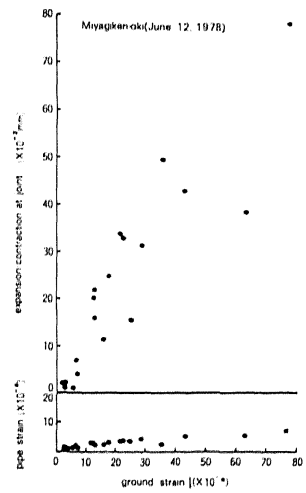

Fig. 10. Relationship between ground strain and pipe strain and expansion-contraction at joint (Shimonaga, point A)

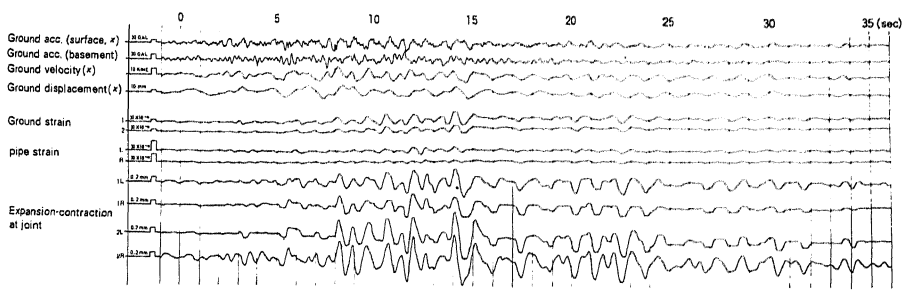

Fig. 9. Recorded waves (Shimonaga, point A, Miyagiken-oki, June 12, 1978)

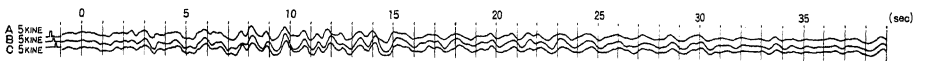

Fig. 11. Velocity waves (Shimonaga, x direction, Miyagiken-oki, June 12, 1978)

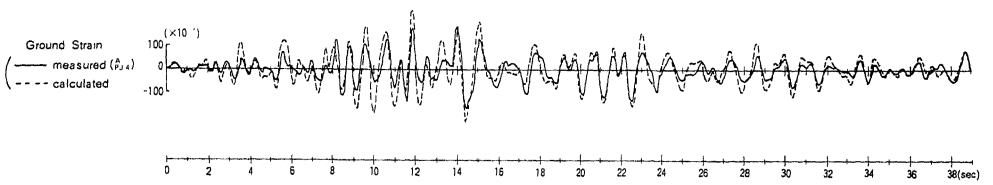

Fig. 12. Comparison between measured ground strain and calculated ground strain by eq.(1) (Shimonaga, Miyagiken-oki, June 12, 1978)

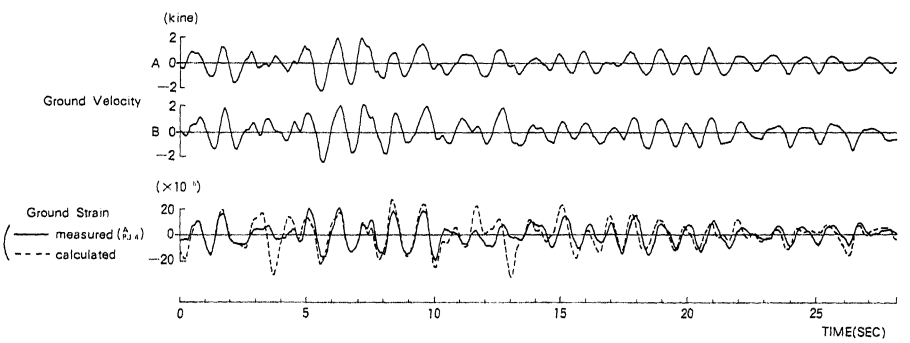

Fig. 13. Comparison between measured ground strain and calculated ground strain by eq.(1) (Shimonaga, Miyagiken-oki, June 14, 1978)

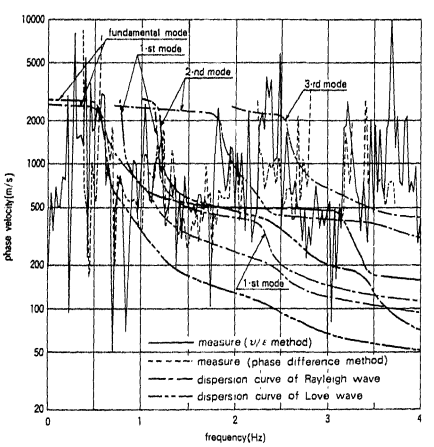

Fig. 14. Comparison between measured phase velocity and dispersion curve of Rayleigh wave, Love wave
(Shimonaga, Miyagiken-oki, June 12, 1978)

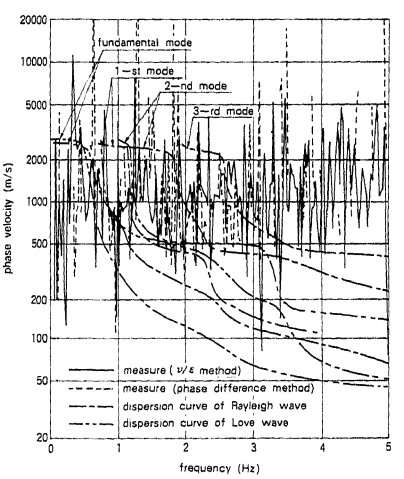

Fig. 15. Comparison between measured phase velocity and dispersion curve of Rayleigh wave, Love wave
(Shimonaga, Miyagiken-oki, June 14, 1978)

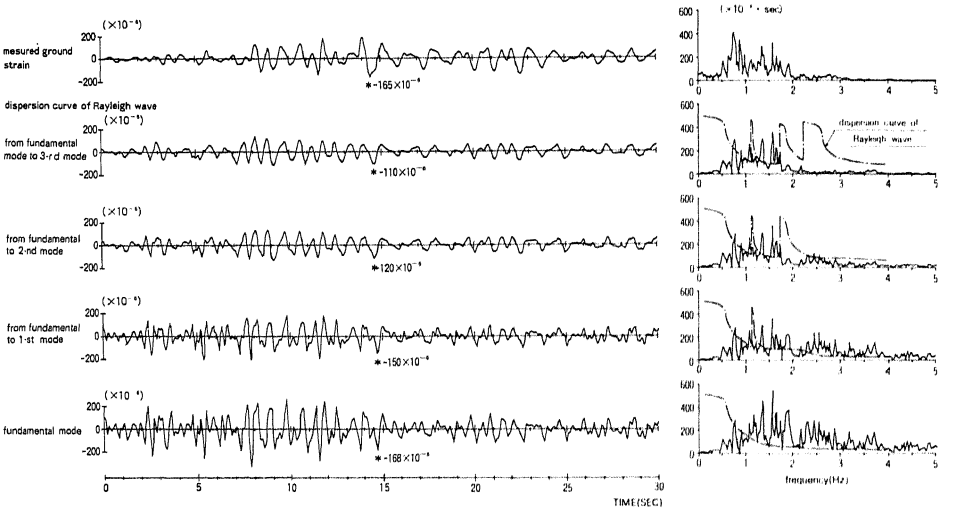

Fig. 16. Comparison between measured ground strain and calculated ground strain of the dispersion curve of the Rayleigh wave (Shimonaga, Miyagiken-oki, June 12, 1978)

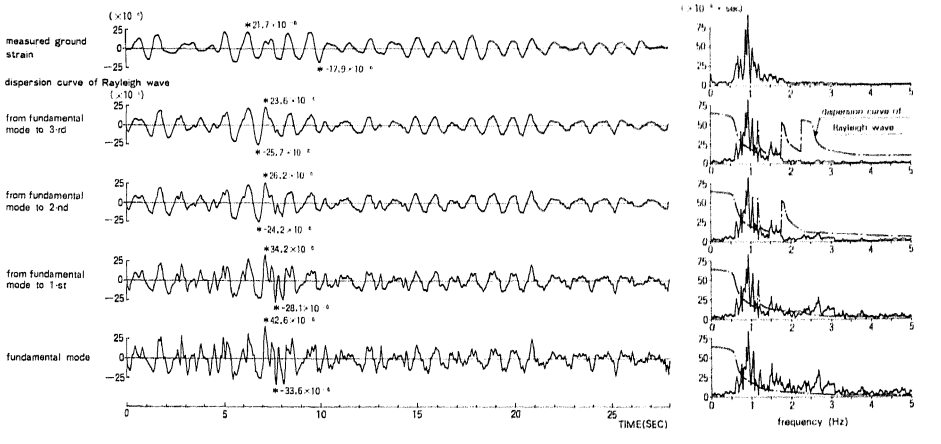

Fig. 17. Comparison between measured ground strain and calculated ground strain of the dispersion curve of the Rayleigh wave (Shimonaga, Miyagiken-oki, June 14, 1978)